



## Comparative study of Rhodamine B and Direct Orange 39 degradation in aqueous solution using atmospheric plasma

César Torres Segundo<sup>a</sup>, Josefina Vergara Sánchez<sup>b,\*</sup>, Esteban Montiel Palacios<sup>a</sup>,  
Aarón Gómez Díaz<sup>c</sup>, Pedro Guillermo Reyes Romero<sup>c</sup>, Horacio Martínez Valencia<sup>d</sup>

<sup>a</sup>Laboratorio de Análisis y Sustentabilidad Ambiental, Escuela de Estudios Superiores de Xalostoc, Universidad Autónoma del Estado de Morelos, Xalostoc, Ayala, Morelos, C.P. 62715, México, emails: cesar.torres@uaem.mx (C.T. Segundo), esteban.montiel@uaem.mx (E.M. Palacios)

<sup>b</sup>Laboratorio de Ingeniería Ambiental, Facultad de Ciencias Químicas e Ingeniería, Universidad Autónoma del Estado de Morelos, Cuernavaca, Morelos, C.P. 62209, México, email: vergara@uaem.mx

<sup>c</sup>Laboratorio de Física Avanzada, Facultad de Ciencias, Universidad Autónoma del Estado de México, Toluca, Estado de México, C.P. 50000, México, emails: agomezd@uaemex.mx (A.G. Díaz), pgrr@uaemex.mx (P.G. Reyes Romero)

<sup>d</sup>Laboratorio de Espectroscopia, Instituto de Ciencias Físicas, Universidad Nacional Autónoma de México, A. P. 48-3, Cuernavaca, Morelos, C.P. 62251, México, email: hm@icf.unam.mx

Received 19 May 2023; Accepted 5 September 2023

### ABSTRACT

The inadequate treatment of industrial wastewater with organic contaminants is a worldwide problem, requiring the development of alternative wastewater treatment methods. This study focused on the degradation and mineralization processes of two dyes, Rhodamine B and Direct Orange 39, in water using atmospheric plasma. Aqueous solutions of the dyes were treated at an initial concentration of 1.0 mM in a volume of 250 mL using iron filings ( $\text{Fe}^{2+}$ ) as a catalyst. Their absorption spectra in the ultraviolet–visible range, total organic carbon, and chemical oxygen demand were monitored. Furthermore, their physicochemical properties such as pH, electrical conductivity, and nitrate and nitrite concentrations were determined. The results showed a process efficiency greater than 90% for both dyes owing to atmospheric plasma exposure.

*Keywords:* Plasma; Textile dye; Nitrate; Nitrite; Optical emission spectroscopy

### 1. Introduction

Population growth increases the need for clean water and creates pressure on the use of water resources. Accordingly, increasing domestic and industrial water use results in the consumption of water resources at an accelerated rate, requiring the treatment of wastewater [1]. Currently, approximately 100,000 dyes are on the market, and 1 million tons of dyes are produced annually. It is estimated that 10% of these dyes are released into the environment without proper treatment [2].

One of the most widely used dyes in the textile and food industries is Rhodamine B (RhB, a xanthene dye). Its

prolonged exposure has adverse effects on animals and humans, such as skin irritation, eye and respiratory tract infection, and chronic and neurotoxicity, in addition to carcinogenicity [3]. Therefore, the European Union and China have prohibited its use. Generating methods for the elimination of RhB, physically, chemically, or biologically, is of high interest [4] as conventional biological treatments are inefficient for the degradation of dyes with a large number of aromatic rings [5].

Direct Orange 39 (DO39) is an azo dye, making its degradation challenging owing to its recalcitrant nature, solubility in water, and the possibility of the generation of intermediate compounds more toxic than the original molecule. This dye inhibits the germination of *Triticum aestivum*

\* Corresponding author.

and *Phaseolus mungo*. Therefore, it is crucial to find effective mechanisms to remove DO39 from effluents to reduce the risks to living organisms and the environment [6].

To find an alternative solution for the elimination of dyes from wastewater, various advanced oxidation processes (AOPs) have been studied using different combinations, such as  $H_2O_2$ /Fenton, ultraviolet (UV)/ $TiO_2$ / $O_3$ / $H_2O_2$ , UV/ $H_2O_2$ , and UV/ $O_3$ , as well as ozonation. AOPs generate hydroxyl radicals ( $OH^\bullet$ ), which is a powerful oxidant with an oxidation potential of approximately 2.86 V. They react with and degrade stable nonbiodegradable organic compounds via hydrogen bond abstraction, electrophilic addition, and electron transfer reactions [7]. However, their efficiency depends on the type of  $OH^\bullet$  precursor, the catalyst used, the turbidity of the solution, the complexity of the system, and the limitations of the mass transfer of reactants. Thus, a better technology is sought to improve the efficiency of the oxidation process [8]. Cold plasma generated at atmospheric pressure is an AOP that offers a promising remediation process for both water and soil with low energy consumption, high pollutant degradation efficiency, short treatment time, and negligible secondary pollution [9].

The degradation of textile dyes from industrial wastewater is a complex process owing to the presence of a large amount of contaminants. Thus, it must be studied in a controlled environment to exclude the formation of intermediate products unrelated to the kinetics of the degradation of the dye under study. To perform this type of research, the dynamic effects of the fluids and the physical characteristics of the plasma used must be considered in addition to the relevant chemistry. The comparison of the application of the same plasma treatment under the same experimental conditions, is a good strategy to understand the changes in the physicochemical variables of the treated solution.

This work investigated the degradation process of two dyes, RhB and DO39, that interacted with a corona-type plasma generated at atmospheric pressure. Both dyes were treated in a batch system, which had an electrode completely submerged in the sample and connected to the physical ground and an upper electrode connected to a high voltage and placed on the surface of the sample, generating plasma at the liquid–air interface [10]. The variables used to monitor the generated plasma include voltage, current, and optical emission spectra. Regarding the sample, the following parameters were measured: dye weight, temperature, volume, pH, absorbance, nitrate and nitrite concentrations, total organic carbon (TOC), and chemical oxygen demand (COD). Based on these parameters, the dye concentration, discoloration factor, mineralization percentage,  $G_{50}$ , and electrical cost were calculated. Our study has the advantage of combining the chemical effects generated using  $Fe^{2+}$  as a catalyst (Fenton process) with the physical treatment (atmospheric plasma).

## 2. Methodology

### 2.1. Experimental system

The plasma reactor used for the degradation is shown in Fig. 1. It had acrylic protection, and the solution container was a beaker Pyrex glass with a capacity of 400 mL. The electrical discharge was generated by applying a voltage

of 2,000 V using a high voltage power supply in direct current (HP Mod. 6,525 A, 4.0 kV–50 mA) at a constant power of 80 W between two tungsten electrodes with a diameter of 3.0 mm aligned to the center of the reactor. The cathode (ground connection) was in the solution, 1.0 cm, and the anode was placed on the surface of the solution. Plasma was produced just above the surface of the sample at the water–air interface. The container was fitted with an optical fiber connected to a spectrometer (StellarNet EPP2000, United States, wavelength range of 200–1,100 nm) to perform optical emission spectroscopy (OES) in real time. The plasma treatment time was between 15 and 60 min for RhB and between 15 and 150 min for DO39.

The dye concentration was 1.0 mM for both RhB and DO39 with an initial volume of 250 mL and an  $Fe^{2+}$  concentration of 1.0 mM. To perform pH and electrical conductivity measurements, a Hach HQ40d potentiometer (United States) was used. A Hach DR3900 spectrophotometer (United States) was used to measure the absorbance in the range of 320–800 nm. COD and TOC were determined using the low-range Hach vials (TNT835 and HACH Nitrite TNT839). The mineralization was monitored as a function of treatment time with the plasma in function of the TOC values. Iron filings ( $Fe^{2+}$  analytical grade) were used as the catalyst and removed from the solution after treatment using filtration. Subsequently, color, COD, and TOC measurements were performed. Sampling was performed every 15 min.

### 2.2. Preparation of dye solutions

#### 2.2.1. RhB solution

RhB (analytical reagent grade, CAS number of 81-88-9) has a molecular weight of 479.02 g/mol, color index of 45,170, and chemical formula of  $C_{28}H_{31}N_2O_3Cl$  (Table 1).

First, RhB was weighed and adjusted to 119.755 mg and dissolved in distilled water. The solution was placed in a volumetric flask. Iron filings ( $Fe^{2+}$ ) were added, and the volume was adjusted to 250 mL. The initial solution contained 1.0 mM RhB and 1.0 mM iron filings. The initial experimental conditions include a temperature of 25°C, a pH of 7.42, and an initial electrical conductivity of 86  $\mu S/cm$ , measured with

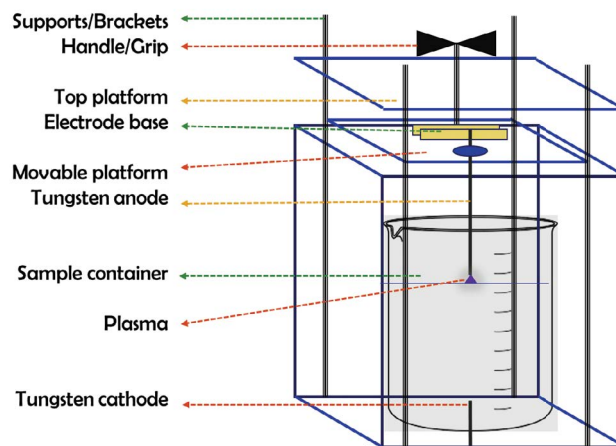


Fig. 1. Atmospheric plasma reactor for the degradation of dyes.

a Hach HQ40d (United States). Absorbance measurements of the RhB solution were collected using a Hach DR3900 spectrophotometer (United States). Specifically, 1.0 mL of the dye solution was obtained, diluted with 2.0 mL of distilled water, and placed in a quartz cell. The main absorbance peak was at 554 nm, and these measurements were used to obtain the dye calibration curve based on the Beer–Lambert law, which allows lineal adjustment to obtain the relation between absorbance and solution concentration. For this dye, the measurements were conducted every 15 min up to a final time of 60 min. All solutions were prepared from analytical-grade chemicals with five repetitions under the same initial conditions.

### 2.2.2. DO39 solution

DO39 is a recalcitrant compound, and its intermediate compounds can be very toxic to aquatic life [6]. It is mainly used in cloth dyeing, printing, and leather and paper shading. It has a molecular weight of 299.28 g/mol, CAS number of 1325-54-8, color index of 40,215, and chemical formula of  $C_{12}H_{10}N_3O_3SNa$  (Table 2).

74.82 mg of DO39 was weighed and dissolved in distilled water in a beaker to obtain an initial solution concentration of 1.0 mM. The solution was placed in a volumetric flask. Iron filings ( $Fe^{2+}$ ) were added with a molar concentration of 1.0 mM, and the volume was adjusted to 250 mL. The initial experimental conditions include a temperature of 25°C, pH of 8.22, and an electrical conductivity of 260  $\mu S/cm$  (Hach HQ40d multiparameter, United States). The absorbance of the DO39 solution was measured using a Hach DR3900 spectrophotometer (United States). Specifically, 1.0 mL of the dye solution was obtained, diluted with 2.0 mL of distilled

water, and placed in a quartz cell. In this case, the characteristic absorbance peak was observed at 444 nm as for dye RhB, the calibration curve that related absorbance and dye concentration. The analysis was performed every 15 for 150 min. All solutions were prepared from analytical-grade chemicals, and the experiment was performed five times under the same initial conditions.

### 2.3. Analysis methods

#### 2.3.1. Dye removal efficiency

The dye removal efficiency,  $\eta$ , was calculated using Eq. (1):

$$\% \text{ of mineralization} = \frac{TOC_0 - TOC_t}{TOC_0} \times 100\% \quad (1)$$

where  $C_0$  is the initial concentration of the dye, and  $C_t$  is the concentration of the dye after plasma treatment, both in mM [15]. The removal efficiency is given in terms of the relationship between the initial concentration of the dye and dye concentrations at different times and determines the performance of the treatment.

#### 2.3.2. Percentage of mineralization

The values of TOC during the atmospheric plasma treatment were used to monitor dye mineralization using the Hach method with low-range vials. The TOC concentration refers to the carbon content of the organic dye and other organic intermediate compounds that were generated during the plasma treatment. An ultraviolet-visible (UV-Vis)

Table 1  
Chemical information of Rhodamine B (RhB) [11,12]

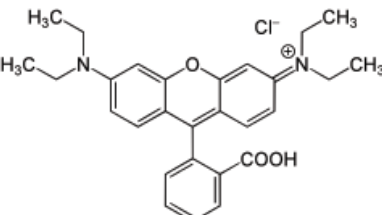
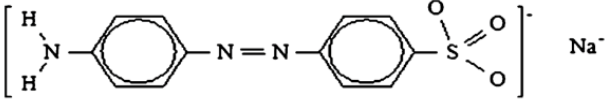
Structure	Characteristic	References
	Color index name	Basic Violet 10
	Chemical formula	$C_{28}H_{31}N_2O_3Cl$
	Chemical class	Xanthene
	Color index number	45,170
	$\lambda_{max}$ (nm)	554
	Molecular weight (g/mol)	479.02
	CAS number	81-88-9

Table 2  
Chemical structure of Direct Orange 39 (DO39) [13,14]

Structure	Characteristic	References
	Color index name	Direct Orange 39
	Chemical formula	$C_{12}H_{10}N_3O_3SNa$
	Appearance	Orange powder
	Color index number	40,215
	$\lambda_{max}$ (nm)	444
	Molecular weight (g/mol)	299.28
	CAS number	1325-54-8

spectrophotometer (Hach, DR3900, United States) was used to determine the TOC. The percentage of mineralization was calculated using Eq. (2) [16]:

$$\% \text{ of mineralization} = \frac{\text{TOC}_0 - \text{TOC}_t}{\text{TOC}_0} \times 100\% \quad (2)$$

The percentage of mineralization determines the amount of the organic compound converted into  $\text{CO}_2$  and  $\text{H}_2\text{O}$  in terms of the ratio of TOC values at different times to the initial TOC value.

### 2.3.3. Energy efficiency ( $G_{50}$ )

To determine the energy efficiency in the degradation process,  $G_{50}$  was calculated using Eq. (3), which provides information about the amount of energy required to degrade the pollutant to 50% of its initial concentration [17]:

$$G_{50} = 1.8 \times 10^6 \frac{C_0 V_0 M}{P t_{50}} \quad (3)$$

where  $C_0$  denotes the initial molar concentration of the dye at  $t = 0$  s,  $V_0$  is the initial volume of the solution treated (L),  $M$  is the molecular weight of the pollutant,  $P$  is the electrical power (W), and  $t_{50}$  is the time required to eliminate 50% of the contaminant. The  $G_{50}$  factor is expressed in g/kWh.

## 2.4. Plasma characterization

### 2.4.1. Optical emission spectroscopy

The optical emission spectrum was analyzed from the luminescence generated by the plasma formed on the surface of the liquid sample using an optical fiber that passed through the sample container and located in front of the place where the luminescence was produced. The fiber is connected to a StellarNet EPP2000 spectrometer (United States) to take measurements in real time in the wavelength range of 200–1,100 nm with an integration time of 1 s. The emission spectra were analyzed to assign chemical species to the peaks. The electron temperature and the electron density

can be calculated using the intensities of two spectral lines, assuming that the population of the emitting levels follows the Boltzmann distribution [18] and that the system has a local thermodynamic equilibrium in a small fraction of the system. Eq. (4) was used to calculate the electron temperature:

$$T_e = \frac{E_m(2) - E_m(1)}{k} \left[ \ln \left( \frac{I_1 \lambda_1 g_m(2) A_m(2)}{I_2 \lambda_2 g_m(1) A_m(1)} \right) \right]^{-1} \quad (4)$$

where  $E_m(i)$  denotes the energy of the upper levels of the lines,  $k$  is the Boltzmann constant,  $g_m(i)$  represents the statistical weights of the upper levels, and  $A_m(i)$  represents their corresponding transition probabilities [19].  $I_1$  and  $I_2$  denote the relative line intensities in questions, and  $\lambda_1$  and  $\lambda_2$  denote the wavelengths of the lines, which were experimentally measured. Using  $T_e$ , the electron density of the plasma was obtained following the Saha–Boltzmann equation [Eq. (5)]; these two quantities are extremely important to characterize the discharge due to electrons that are responsible for ionization, dissociation, and recombination processes in water.

$$n_e = 6 \times 10^{21} (T_e)^{3/2} \left( \exp \left[ -\frac{E_i}{kT_e} \right] \right) \quad (5)$$

where  $T_e$  denotes the electron temperature,  $E_i$  is the ionization energy of the species, and  $k$  is the Boltzmann constant [20–22].

## 3. Results

Fig. 2A shows the evolution of the absorbance spectra of the samples at different plasma treatment times. As a reference, the maximum absorption peak at 554 nm was used. Notably, a decrease of 27.9%, 59.5%, 96.1%, and 99.8% was obtained at 15, 30, 45, and 60 min. Fig. 2B shows the discoloration associated with the decrease in the absorbance spectra. This discoloration is due to the interaction of free radicals, which are generated during the interaction of the plasma with the sample, resulting in the breakage of nitrogen double bonds (chromophores) responsible for

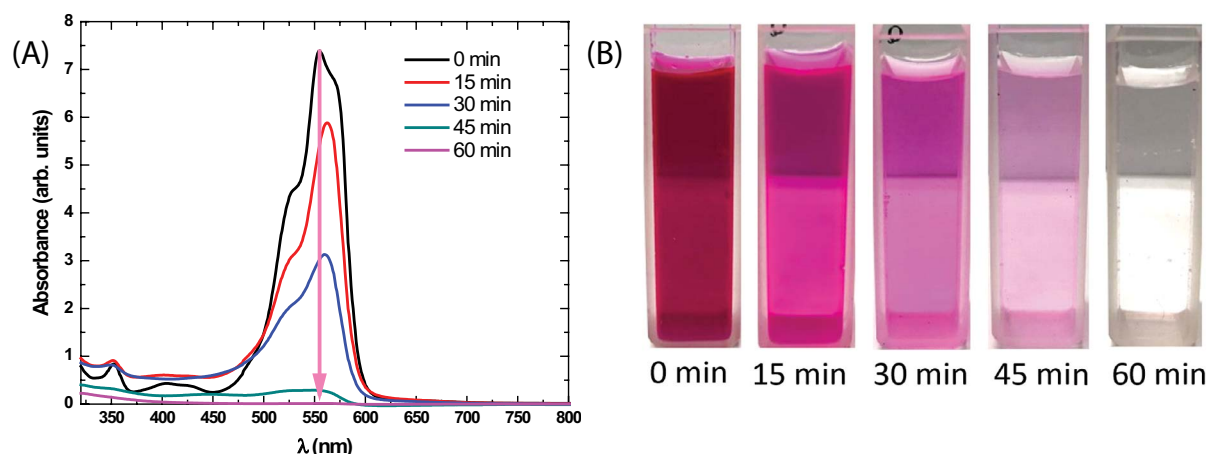


Fig. 2. (A) Absorbance collected at different treatment times of water with RhB. (B) Photographs of the discoloration process.

dye color. Therefore, the dye degradation efficiency of the treatment can be established using these spectra.

Regarding the treatment with DO39, Fig. 3A presents the absorbance of the solution at different times (0–150 min) with their characteristic maximum absorption peak at 444 nm. After 150 min of interaction between the corona discharge and the sample, the absorbance decreased by more than 98% owing to the breakdown of the chromophore group due to the interaction with free radicals. Fig. 3B shows small amounts of the solution as a function of treatment time, where the discoloration was observed: the initial solution had an orange color; at 15 min, the color intensity decreased; at 45 min, the color changed to yellow; at 105 min, the color was still slightly yellow; after 135 min, the solution was colorless. After 150 min, a small amount of radiation was observed below 450 nm, absorbed by the sample, inferring that it is due to the byproducts of the dye preparation process.

The removal efficiency of RhB calculated using Eq. (1) is shown in Fig. 4A; it reached 47.9%, 79.5%, and 96.1% in 15, 30, and 45 min, respectively. Finally, in 60 min, an efficiency of 99.8% was obtained.

Further, using Eq. (1), the removal efficiency of DO39 was obtained, as shown in Fig. 4B. The growth rates in

the first 15, 30, and 45 min were 23.8%, 18.4%, and 16.6%, respectively, with a mineralization of 70.03% at 60 min. However, a treatment time of at least 105 min was required to achieve a percentage of mineralization greater than 90%. The absorbance graphs, the photos of the samples in the discoloration process, and the removal efficiency results showed that under the same experimental conditions, DO39 is more resistant to degradation than RhB, which is expected for Azo-type dyes.

For RhB, the initial values of pH and electrical conductivity (Fig. 5A) were 7.42 and 86  $\mu\text{S}/\text{cm}$ , respectively. After 60 min of treatment, the pH and electrical conductivity values were 3.70 and 417  $\mu\text{S}/\text{cm}$ , respectively, with a 50.1% decrease in the pH value and a 4.8-fold increase in the electrical conductivity. For DO39, the initial pH value was 8.22, and the electrical conductivity was 260  $\mu\text{S}/\text{cm}$  (Fig. 5B), after 150 min, the final pH and electrical conductivity values were 2.68 and 630  $\mu\text{S}/\text{cm}$ , respectively. Generally, during the treatment, a 67.4% decrease in the pH value and a 2.4-fold increase in the electrical conductivity value were observed for the DO39 solution.

The decrease in pH can be explained using reaction 1 [23] owing to the increase in the concentration of  $\text{H}^+$ , which led

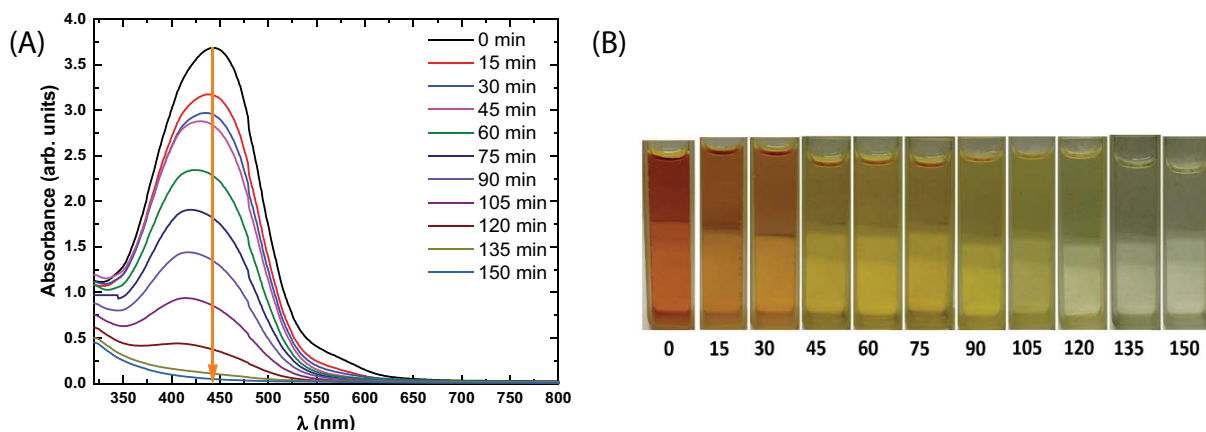


Fig. 3. (A) Absorbance collected at different treatment times of water with DO39. (B) Photographs of the discoloration process.

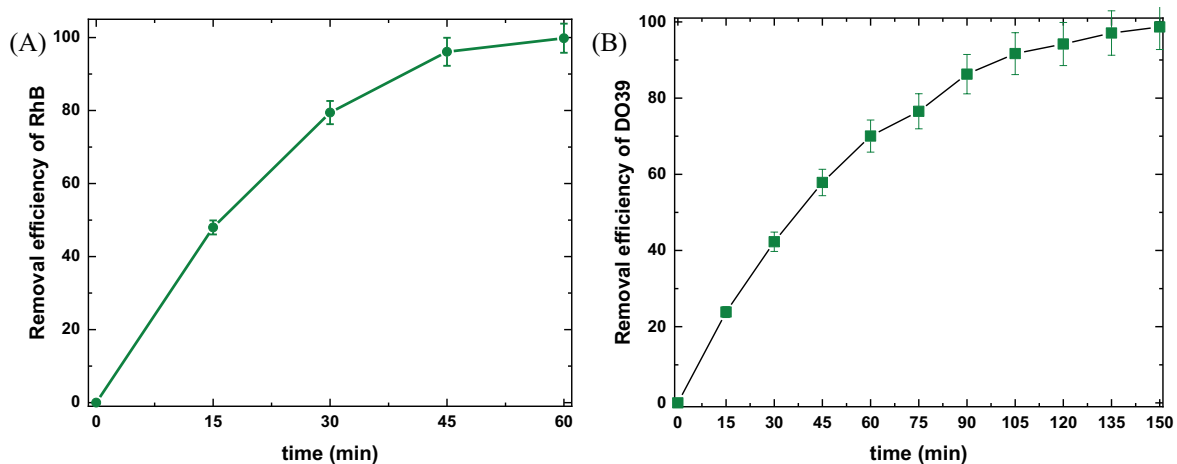
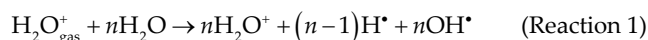
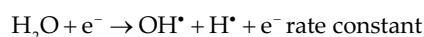


Fig. 4. (A) Removal efficiency of RhB vs. treatment plasma time. (B) Removal efficiency of DO39 vs. treatment plasma time.

to an increase in the electrical conductivity of the solution simultaneously. These changes were similar for both dyes.



When the plasma interacts with the solution, pH and electrical conductivity values are affected because the system is supplied with high-energy electrons, reaction 2 [24,25], causing the ionization, dissociation, and recombination of water molecules, which generate OH\* and H\* radicals. Thus, the recombination of OH\* radicals in the solution produces hydrogen peroxide, reaction 3 [26]:

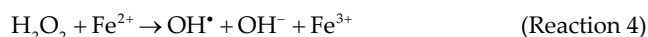


$$k = 2.3 \times 10^{-12} - 1.8 \times 10^{-10} \frac{\text{cm}^3}{\text{s}} (T_e = 1 - 2 \text{ eV}) \quad (\text{Reaction 2})$$

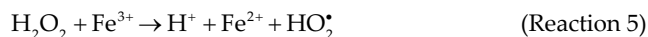


$$\text{rate constant } k = 4 \times 10^{-9} \frac{\text{cm}^3}{\text{s}} \quad (\text{Reaction 3})$$

Iron filings were used as the catalyst to convert hydrogen peroxide into hydroxyl radicals (reaction 4) [24].



Besides, Fe<sup>3+</sup> is transformed into Fe<sup>2+</sup> by consuming the hydrogen peroxide generated by the plasma.



Considering reactions 1–5, the generation of hydroxyl radicals can break organic bounds and mineralize the initial compound and its by-products, as described by reactions 6 and 7 [24].



Regarding the TOC and COD behaviors of RhB and DO39, Fig. 6A and B, respectively, show that they decreased as a function of treatment time in both cases. The initial values of these RhB parameters were 336 mg/L for TOC and 48 mg/L for COD, indicating a 48% decrease at 15 min for both parameters. The final values at 60 min were 0.64 and

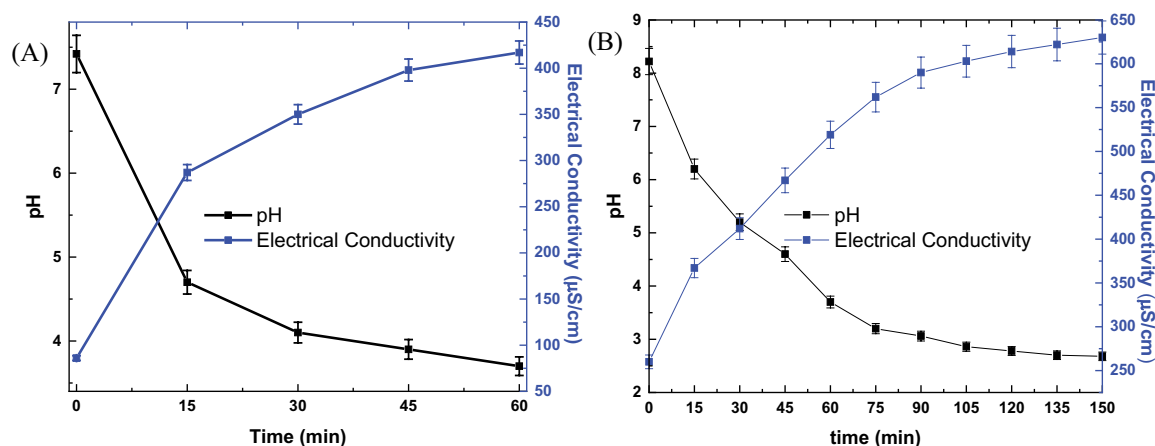


Fig. 5. (A) pH and electrical conductivity as a function of time during the treatment of RhB. (B) pH and electrical conductivity during the treatment of DO39.

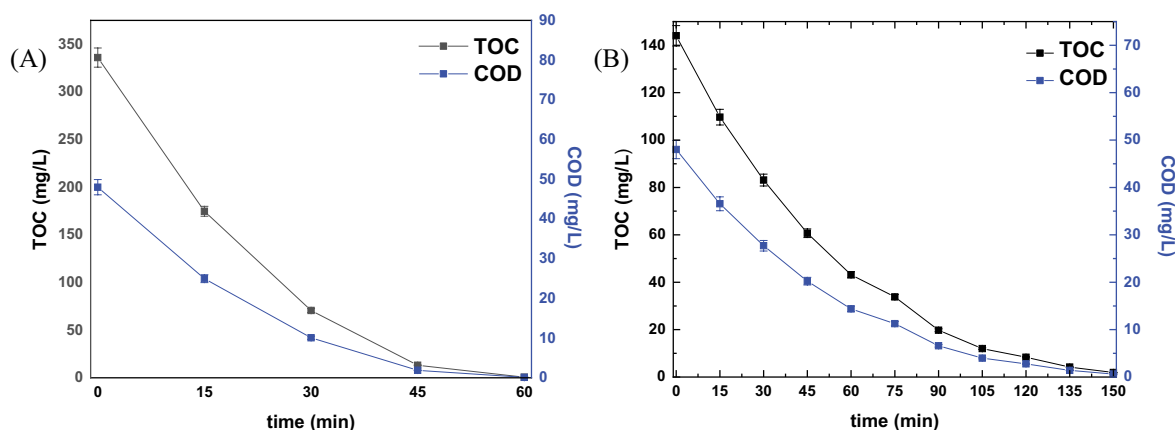


Fig. 6. Behaviors of COD and TOC vs. time for (A) RhB and (B) DO39.

0.09 mg/L for TOC and COD, respectively. For DO39, the TOC and COD values were 144 and 48 mg/L, respectively, indicating a 23.8% decrease at 15 min for both parameters; after 150 min of treatment, these parameters were 6.3 and 2.9 mg/L, respectively.

Fig. 7 shows the percentage of mineralization calculated using Eq. (2). The RhB growth rates in the first 15, 30, and 45 min were 48%, 31%, and 17%, respectively; achieving 98% mineralization in 60 min. For DO39, the growth rates in 15, 30, and 45 min were 23.8%, 18.4%, and 16.6%, respectively. At 60 min, a mineralization of 70.0% was obtained. However, to have a percentage of mineralization greater than 90%, a treatment time of at least 105 min was required.

Furthermore, in this paper, the values of the parameters for RhB were  $C_0 = 0.001$  M,  $V_0 = 0.25$  L,  $M = 479.02$  g/mol,  $P = 80$  W, and  $t_{50} = 948$  s. Using these values in Eq. (3), a  $G_{50}$  value of 2.84 g/kWh was obtained, which is comparable to

those reported in other articles (Table 3). Also, for DO39, the initial dye concentration is at  $C_0 = 0.0001$  M, initial volume is at  $V_0 = 0.25$  L,  $M = 299.28$  g/mol, electric power is at  $P = 80$  W, and time at  $t_{50} = 2040.6$  s. These values, when substituted into Eq. (3), yielded a  $G_{50}$  value of 0.825 g/kWh.

Table 3 shows that the  $G_{50}$  value obtained in this work is higher than most of those reported in [8,27–30]. For its part, the  $G_{50}$  value of RhB was 3.4 times that of DO39.

By augmenting the treatment time, other reactive oxygen (ROS) and nitrogen (RNS) species are generated. Furthermore, acids (inorganic and carboxylic) are produced, which decrease the pH and increase the electrical conductivity (Fig. 5). Fig. 8 shows that the concentrations of nitrites and nitrates increase with longer plasma exposure times, as reported previously [31–33]. These anions are produced during the reaction of the dissociated  $N_2$  molecules with  $O_2$  or  $H_2O$  in the gas phase and their subsequent dissolution in the aqueous solution of the dye.

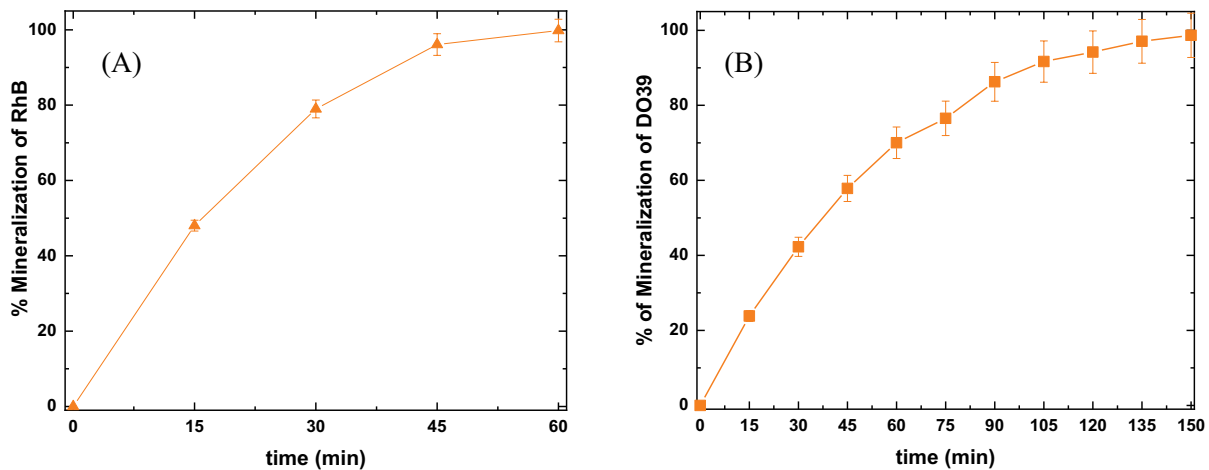


Fig. 7. Percentage of mineralization of (A) RhB and (B) DO39 by plasma vs. time.

Table 3

$G_{50}$  values obtained during the degradation of Rhodamine B using various AOPs

Dye	AOPs	$G_{50}$ (g/kWh)	References
RhB	Pulsed-SSD in water	0.081	[8]
RhB	Pulsed-SSD in water	0.202	[8]
RhB	Streamer discharge	0.025	[27]
RhB	Spark discharge	0.080	[27]
RhB	Spark–streamer mixed discharge modes	0.160	[27]
RhB	UV/H <sub>2</sub> O <sub>2</sub>	0.1	[8]
RhB	Ultrasound	0.2	[8]
RhB	Photocatalysis	0.2	[8]
RhB	Hydrodynamic cavitation	0.01	[8]
RhB	Ozonation	0.3	[8]
Methyl orange	Corona	0.45	[28]
Methyl orange	Glow discharge	0.024	[29]
Methylene blue	Jet	0.296	[30]
RhB	Corona discharge	2.84	[31]
Direct Orange 39	Corona discharge	0.825	[32]

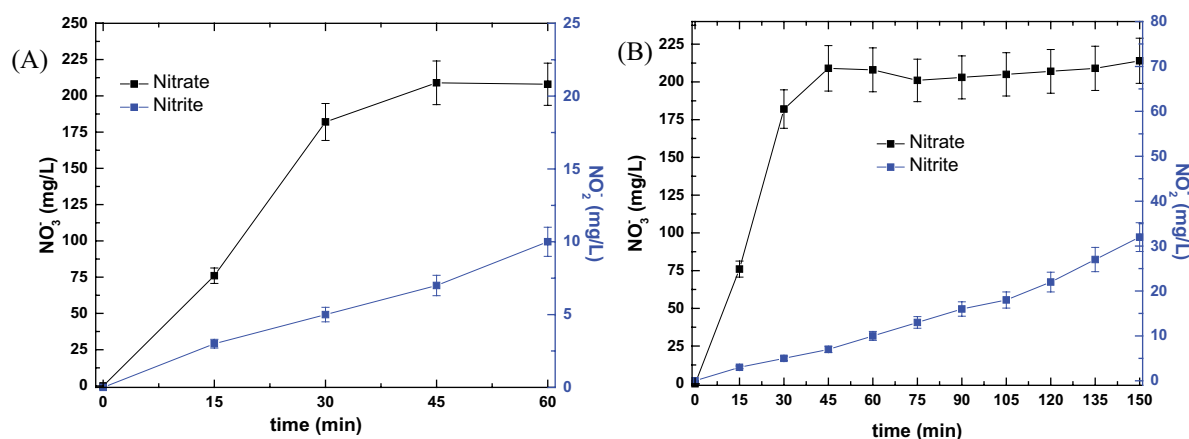


Fig. 8. Nitrate and nitrite concentrations in the solution during the plasma treatment of (A) RhB and (B) DO39 vs. time.

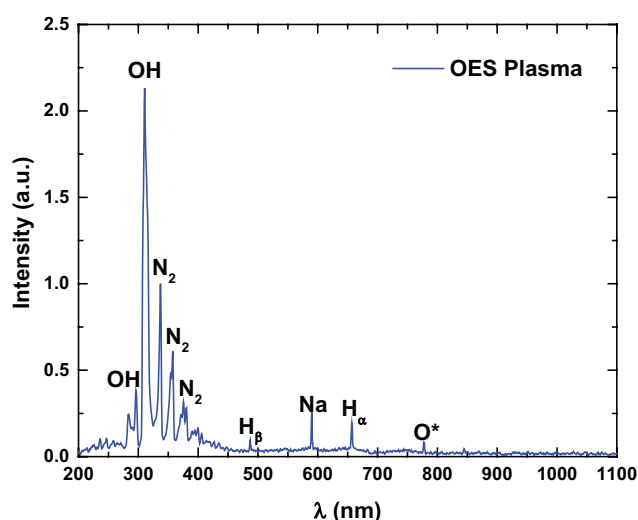


Fig. 9. OES of the corona discharge used for mineralization.

Fig. 8 shows that the nitrate concentration increased in the first 45 min of treatment; then, it remained constant. Conversely, the nitrite concentration increased during the 60 min of plasma exposure. The initial concentrations of both anions were zero, so the presence of these species in the aqueous solution is directly related to the plasma treatment.

Fig. 9 shows the OES result obtained during RhB degradation, which is comparable to that reported by Torres for DO39 [31,32]. It was normalized for  $N_2$  since plasma was produced in an air atmosphere, whose main component is nitrogen. The intensity of the OH emission band located at 309.5 nm was greater than that of nitrogen at 337 nm owing to the greater amount of oxygen present in the solvent and in the dye.

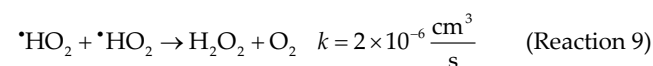
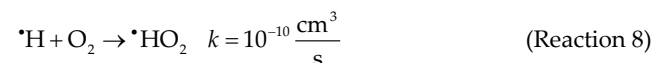
Fig. 9 shows the OES result of the corona discharge in air generated during the RhB degradation process. Emission lines corresponded to different excited species ( $H_{\alpha}$ ,  $H_{\beta}$ ,  $N_2$ , OH, and Na). The detailed assignments are given in Table 4. In addition, the sodium doublet (D-lines) was recognized, which is frequently observed in the spectra of degradation processes.

Table 4  
Main species detected using OES during corona discharge treatment

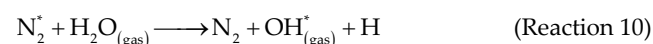
Species	$\lambda$ (nm)	Transition	Energy (eV)
OH	284.0		3,064 Å system
	309.5		
$N_2$	337.0		Second positive system
	357.5		
	375.5		
	380.5		
$H_{\beta}$	487.0	2–4	2.5497
Na	590.0		2.1023
$H_{\alpha}$	656.5	2–3	1.8887
$O^*$	777	$3p^5P \rightarrow 3s^5S$	1.8427

The electrons provided by the plasma that is generated on the water surface can dissociate  $H_2O$  molecules. Then, in the bulk solution, a chain reaction can produce  $H_2O_2$  molecules, which react with other species and produce  $OH^*$  radicals.

Hydrogen atoms, hydroxyl radicals, and hydrogen peroxide molecules have been reported to be produced at the plasma–liquid interface owing to the reciprocal action between the corona discharge and the water surface. The main reactions are shown in reactions 2, 3, 8, and 9 [25]:



Hydroxyl radicals can be produced by reactions 2 and 10. The corona discharge in air produces excited molecular nitrogen. In reaction 10, the reaction of excited molecular nitrogen with water vapor from the air generates  $OH^*$  [30], a highly oxidizing species that can degrade and even mineralize most of the organic contaminants present in water:





The temperature and electron density were determined to characterize the corona discharge applied during the degradation process. The electronic temperature was 2.4 eV, obtained by substituting the values of  $H_{\alpha}$  and  $H_{\beta}$  in Eq. (4). The electronic density of the plasma was  $5.69 \times 10^{12}$  particles/cm<sup>3</sup>, obtained using Eq. (5) by considering the values of the electronic temperature and the ionization energy of hydrogen.

An important factor to consider in wastewater treatment is the cost. In this study, only the cost of electrical energy consumption is considered because it is much higher than other costs, such as the cost related to electrode wear. The cost of electrical energy can be determined using Eq. (6) [34]:

$$\text{Electric cost} = \frac{U \times I \times t_{\text{treatment}}}{V} \quad (6)$$

where  $U$  is the voltage applied to generate plasma (V),  $I$  is the current intensity (A),  $t_{\text{treatment}}$  is the treatment time (h), and  $V$  is the volume of the treated water (m<sup>3</sup>). The cost of electricity is expressed in USD/kWh (in Mexico, the price of electricity is 0.04 US dollars per kWh). In this study, the values of the variables used were  $U = 1,000$  V,  $I = 0.08$  A,  $t_{\text{treatment}} = 1$  h, and  $V = 2.5 \times 10^{-4}$  m<sup>3</sup>. The cost of treating 1 m<sup>3</sup> of the aqueous solution of RhB was found to be 3.20 USD. Under similar conditions, the cost of treating 1 m<sup>3</sup> of the aqueous solution of DO39 was \$1.28/m<sup>3</sup>; based on this comparison, the treatment of the solution with RhB is cheaper. The cost of plasma treatment is lower than other treatment methods, such as Fenton and photo-Fenton methods, which use expensive chemical reagents.

The use of chemical agents during the treatment of water with organic contaminants substantially increases the cost, and this occurs in other AOPs, where an iron sulfate catalyst is used in an acid solution. For a similar treatment with another dye, 5.0 mL of FeSO<sub>4</sub> in an acid solution was used for every 250 mL of the solution. However, upon extrapolating the values for 1 m<sup>3</sup>, it would be necessary to use 20 L of the catalyst, ~278 g of iron sulfate with an approximate cost of \$60, 110 mL of sulfuric acid that would cost ~\$2, and distilled water that would cost \$10, amounting to ~\$72. Thus, in this work, iron filings were used as the catalyst, and the cost of the treatment was related to the electrical energy used.

The main drawbacks of batch treatment include electrical energy consumption and an increase in treatment time with the volume of treated water. However, our study provides basic knowledge that can overcome these drawbacks. We recommend the use of continuous-flow wastewater treatment systems, as they can treat much larger volumes of water than batch systems. In addition, the use of a heterogeneous catalyst facilitates its separation from the aqueous solution and allows its reuse.

#### 4. Conclusions

A degradation efficiency greater than 50% was obtained at plasma treatment times of 15 and 45 min for RhB and DO39, respectively, showing that the proposed treatment method can be applied in combination with another treatment for low colorant concentrations. For DO39, the COD and TOC were reduced by 98.6% and 98.7% at 150 min,

respectively. At the same time, a mineralization percentage of 98.5% was achieved. In the case of RhB, the percentage of mineralization of Rhodamine B was 99% after 60 min of treatment, and the COD and TOC removal were 99.8%. In both cases, the use of iron filings as the catalyst accelerates the degradation process and facilitates dye mineralization.

The concentrations of nitrates and nitrites were 214 and 32 mg/L for DO39, and they were 208 and 10 mg/L for RhB at 150 min, respectively, indicating that the treatment generates high levels of nitrates and nitrites in the water, which is desirable for its application in agriculture for vegetable cultivation.

The energy yield value ( $G_{50}$ ) was 1.99 g/kWh for RhB and 0.825 g/kWh for DO39, indicating that the complexity of the contaminant to be removed decreases this value. The electrical cost calculated for the treatment of a cubic meter of water with the dyes using plasma was found for be few dollars, which may allow the deployment of the treatment method to the mineralization of organic compounds in large volumes of wastewater. From the optical spectrum of plasma emission, the principal species identified were OH, N<sub>2</sub>, Na, H<sub>α</sub>, and H<sub>β</sub>.

#### Acknowledgments

This research was supported by DGAPA IN105519, PRODEP DSA/103.5/15/6986, PROMEP 103.5/13/6626, PRODEP CA-5511-6/18-8304, PII-43/PIDE/2013, CONACyT 268644, and UAEMex 6743/2022CIB.

#### References

- [1] L. Hakan, A. Gündüz, R. Atav, S. Soysal, F. Yıldız, Investigation of the treatment of textile wastewater with cold atmospheric plasma reactor (Profoks) and reuse of recycled water in reactive dyeing process of cotton, *J. Nat. Fibers*, 19 (2022) 1–14.
- [2] J.P. Jadhav, S.S. Phugare, R.S. Dhanve, S.B. Jadhav, Rapid biodegradation and decolorization of Direct Orange 39 (Orange TGLL) by an isolated bacterium *Pseudomonas aeruginosa* strain BCH, *Biodegradation*, 21 (2010) 453–463.
- [3] S. Meiyazhagan, S. Yugeswaran, P.V. Ananthapadmanabhan, P.R. Sreedevi, K. Suresh, Relative potential of different plasma forming gases in degradation of Rhodamine B dye by microplasma treatment and evaluation of reuse prospectus for treated water as liquid fertilizer, *Plasma Chem. Plasma Process.*, 40 (2020) 1267–1290.
- [4] Y. Chen, Y. Li, X. Zhang, A. Zhu, Y. Huang, Z. Liu, K. Yan, Degradation of aqueous Rhodamine B with gaseous streamer corona plasma, *IEEE Plasma Sci.*, 43 (2015) 828–835.
- [5] M. Magureanu, D. Piroi, N.B. Mandache, V. Parvulescu, Decomposition of methylene blue in water using a dielectric barrier discharge: optimization of the operating parameters, *J. Appl. Phys.*, 104 (2008) 103306, doi: 10.1063/1.3021452.
- [6] L.A.S.J. Carvalho, R.A. Konzen, A.C.M. Cunha, P.R. Batista, F.J. Bassetti, L.A. Coral, Efficiency of activated carbons and natural bentonite to remove Direct Orange 39 from water, *J. Environ. Chem. Eng.*, 7 (2019) 103496, doi: 10.1016/j.jece.2019.103496.
- [7] A. Kumar, N. Škoro, W. Gernjak, D. Povrenović, N. Puač, Direct and indirect treatment of organic dye (Acid Blue 25) solutions by using cold atmospheric plasma jet, *Front. Phys.*, 10 (2022) 835635, doi: 10.3389/fphy.2022.835635.
- [8] M.I. Stefan, *Advanced Oxidation Processes for Water Treatment: Fundamentals and Applications*, IWA Publishing, United Kingdom, 2018.
- [9] Ch.A. Aggelopoulos, Recent advances of cold plasma technology for water and soil remediation: a critical review, *Chem. Eng. J.*, 428 (2022) 131657, doi: 10.1016/j.cej.2021.131657.

- [10] C. Torres, J. Vergara, P.G. Reyes, A. Gómez, M.J. Rodríguez, H. Martínez, Effect on discoloration by nonthermal plasma in dissolved textile dyes: Acid Black 194, *Rev. Mex. Ing. Quim.*, 18 (2019) 939–947.
- [11] R. Sabarish, G. Unnikrishnan, Novel biopolymer templated hierarchical silicalite-1 as an adsorbent for the removal of Rhodamine B, *J. Mol. Liq.*, 272 (2018) 919–929.
- [12] J. Gu, Ch. Luo, W. Zhou, Z. Tong, H. Zhang, P. Zhang, X. Ren, Degradation of Rhodamine B in aqueous solution by laser cavitation, *Ultrason. Sonochem.*, 68 (2020) 105181, doi: 10.1016/j.ultsonch.2020.105181.
- [13] Z.M. Fard, M. Bagheri, S. Rabieh, H.Z. Mousavi, Synthesis of hierarchical RGO@Cu<sub>2</sub>O@Cu nanocomposites: optimization of photocatalytic degradation of Direct Orange 39 using a response surface methodology, *J. Mater. Sci. - Mater. Electron.*, 13 (2017) 1–9.
- [14] M. Muruganandham, J. Yang, J.J. Wu, Effect of ultrasonic irradiation on the catalytic activity and stability of goethite catalyst in the presence of H<sub>2</sub>O<sub>2</sub> at acidic medium, *Ind. Eng. Chem. Res.*, 46 (2007) 691–698.
- [15] J. Fan, H. Wu, R. Liu, L. Meng, Z. Fang, F. Liu, Y. Xu, Non-thermal plasma combined with zeolites to remove ammonia nitrogen from wastewater, *J. Hazard. Mater.*, 401 (2021) 123627, doi: 10.1016/j.jhazmat.2020.123627.
- [16] P.M.K. Manoj Kumar Reddy, B. Ramaraju, C. Subrahmanyam, Degradation of malachite green by dielectric barrier discharge plasma, *Water Sci. Technol.*, 67 (2013) 1097–1104.
- [17] M.A. Malik, Water purification by plasmas: which reactors are most energy efficient?, *Plasma Chem. Plasma Process.*, 30 (2010) 21–31.
- [18] G.G. Raju, Feature article—collision cross sections in gaseous electronics part I: what do they mean?, *IEEE Electr. Insul. Mag.*, 22 (2006) 5–23.
- [19] NIST, Available at: <https://www.nist.gov/>
- [20] V.K. Unnikrishnan, K. Alti, V.B. Kartha, C. Santhosh, G.P. Gupta, B.M. Suri, Measurements of plasma temperature and electron density in laser-induced copper plasma by time-resolved spectroscopy of neutral atom and ion emissions, *Pramana J. Phys.*, 74 (2010) 983–993.
- [21] H.R. Griem, *Principles of Plasma Spectroscopy*, Cambridge University Press, United Kingdom, 1997.
- [22] J. Feng, Z. Wang, Z. Li, W. Ni, Study to reduce laser induced breakdown spectroscopy measurement uncertainty using plasma characteristic parameters, *Spectrochim. Acta*, 65 (2010) 549–556.
- [23] J. Xing-long, W. Xiao-yan, W. Qing-Feng, Y. Jun-jie, C. Ya-qi, Plasma degradation of cationic blue dye with contact glow discharge electrolysis, *Water Sci. Technol.*, 62 (2010) 1457–1463.
- [24] B. Jiang, J. Zheng, S. Qiu, M. Wu, Q. Zhang, Z. Yan, Q. Xue, Review on electrical discharge plasma technology for wastewater remediation, *Chem. Eng. J.*, 236 (2014) 348–368.
- [25] H. Ghodbane, O. Hamdaoui, J. Vandamme, J.V. Van Durme, P. Vanraes, C. Leys, A.Y. Nikiforov, Degradation of AB25 dye in liquid medium by atmospheric pressure non-thermal plasma and plasma combination with photocatalyst TiO<sub>2</sub>, *Open Chem.*, 13 (2015) 325–331.
- [26] Ch. Sarangapani, N.N. Misra, V. Milosavljevic, P. Bourke, F. O'Regan, P.J. Cullen, Pesticide degradation in water using atmospheric air cold plasma, *J. Water Process Eng.*, 9 (2016) 225–232.
- [27] A.T. Sugiarto, S. Ito, T. Ohshima, M. Sato, J.D. Skalny, Oxidative decoloration of dyes by pulsed discharge plasma in water, *J. Electrostat.*, 58 (2003) 135–145.
- [28] M. Rahimpour, H. Taghvaei, S. Zafarnak, M.R. Rahimpour, S. Raeissi, Post-discharge DBD plasma treatment for degradation of organic dye in water: a comparison with different plasma operation methods, *J. Environ. Chem. Eng.*, 7 (2019) 103220, doi: 10.1016/j.jece.2019.103220.
- [29] X. Wang, M. Zhou, X. Jin, Application of glow discharge plasma for wastewater treatment, *Electrochim. Acta*, 83 (2012) 501–512.
- [30] M.C. García, M. Mora, D. Esquivel, J.E. Foster, A. Roder, C. Jiménez-Sanchidrián, F.J. Romero-Salguero, Microwave atmospheric pressure plasma jets for wastewater treatment: degradation of methylene blue as a model dye, *Chemosphere*, 180 (2017) 239–246.
- [31] J. Vergara Sánchez, C. Torres Segundo, E. Montiel Palacios, A. Gómez Díaz, P.G. Reyes Romero, H. Martínez Valencia, Removal efficiency of Rhodamine B dye by atmospheric plasma, *Desal. Water Treat.*, 256 (2022) 328–336.
- [32] C. Torres Segundo, J. Vergara Sánchez, E. Montiel Palacios, A. Gómez Díaz, P.G. Reyes Romero, H. Martínez Valencia, Discoloration and mineralization of Direct Orange 39 textile dye in water by atmospheric plasma and ferrous ion, *Desal. Water Treat.*, 226 (2021) 362–371.
- [33] R. Zhou, X. Zhang, J. Zhuang, S. Yang, K. Bazaka, K. Ostrikov, Effects of atmospheric-pressure N<sub>2</sub>, He, air, and O<sub>2</sub> microplasmas on mung bean seed germination and seedling growth, *Sci. Rep.*, 6 (2016) 32603, doi: 10.1038/srep32603.
- [34] D. Ghosh, C.R. Medhi, H. Solanki, M.K. Purkait, Decolorization of crystal violet solution by electrocoagulation, *J. Environ. Prot. Sci.*, 2 (2008) 25–35.